COMBUSTION SYNTHESIS AND CHARACTERIZATION OF NANOSIZED POWDER $SrAl_2O_4:Eu^{2+}$ PHOSPHOR

S. C. M. Calyn[1], M. Nazarov [1,2], A. Nor Nazida[1], and M. N. Ahmad-Fauzi [1*]

[1] School of Materials and Mineral Resources Engineering, University Sains Malaysia, Engineering Campus, 14300 Nibong Tebal, Pulau Pinang, Malaysia
[2] Institute of Applied Physics, Academiei str. 5, Chisinau, MD-2028 Republic of Moldova
**e-mail: afauzi@eng.usm.my*

(Received 20 April 2012)

Abstract

A stoichiometric $SrAl_2O_4:Eu^{2+}$ nanosized powder was synthesized by combustion synthesis using urea at 500°C. The crystal structure, element and phase composition, and particle size were analyzed with the aim to study the properties of nanosized $SrAl_2O_4:Eu^{2+}$ green phosphor and its application. X-ray Diffraction pattern revealed that the $SrAl_2O_4:Eu^{2+}$ crystallizes were a major phase, and $Sr_4Al_{14}O_{25}$ as a secondary phase with a small amount of the dopant has no effect on the crystal structure of $SrAl_2O_4$. Crystalline structure can be observed and enhanced by calcination at 1000ºC with 2-h soaking time in a reductive atmosphere. Nucleation of particles occurs and forms a needle-like structure for $SrAl_2O_4$ and a star-like structure for $SrAl_2O_4:Eu^{2+}$. This structure is unstable and agglomerates during calcination at 1000°C to form a stable specific flower-like structure which enhances the glowing effect of the samples.

1. Introduction

Strontium aluminate oxides are commonly prepared by the conventional solid state reactions (SSR) which require a long reaction time of 2-6 h in a high temperature range of 1200-1600°C. Furthermore, high calcination temperature are also required to induce sintering and aggregation of particles. Milling process was also required in SSR resulting in a reduction of the particle size and a decrease in the luminescent properties. However, by using combustion synthesis, phosphor powders can be prepared in a simpler, safer, more energy saving way and within a shorter time [1]. Combustion synthesis can produce more homogeneous products compared to the solid state reaction method due to good mixing of starting materials and relatively low reaction temperature [2]. There are numerous publications; some of them referring to the combustion synthesis are shown in Table 1.

Theoretically, an ideal combustion is a process in which all the fuel burns completely. It involves burning the entire carbon (C) to carbon dioxide (CO_2), the entire hydrogen (H) to water vapor (H_2O) and all the nitrates (NO_3) to nitrogen (N_2) or nitrogen dioxide (NO_2). Combustion synthesis process has low temperatures, fast heating rate, and short characteristic reaction time. It has been widely used as an efficient and facile method for synthesizing and processing advanced ceramics (structural and functional), catalysts, composites, alloys, intermetallics, and nanomaterials [9]. It also plays an important role to produce complex oxides ceramics, such as aluminates, ferrites, and chromites [10]. Combustion synthesis route provides low density mass reducible to very fine particles up to submicron region. Oxidizing atmosphere prevails in combustion process [5]. The concept of combustion synthesis is the exothermicity of redox

(reduction-oxidation or electron transfer) chemical reaction between metal nitrate precursor and a fuel like urea at a relatively low temperature. The excessive heat required during combustion process completes in the reaction in short time producing small particles with high crystallinity. Combustion synthesis can be divided depending on the nature of the reactants: elements or compounds (solid, liquid, or gas) and the exothermicity (adiabatic temperature). The advantages of the combustion synthesis are the following [9]: simple usage of equipment, high purity products, stabilization of metastable phases, and the formation of products with nearly any size and shape. Useful oxide materials can be prepared by a rapid heating of aqueous solutions containing metal nitrates (oxidizer) and fuels like urea/hydrazides [carbon hydrazine (CH), oxalyl dihydrazide (ODH), malonic acid dihydrazide (MDH), tetra formal tris azine (TFTA), etc.]. The purposes of using fuels are as follows: they are a source of C and H, which will combust to form CO_2 and H_2O and liberating heat, they form complexes with the metal ions providing a homogeneous mixture of cations in solution or gel.

Table 1. Comparison of properties of $SrAl_2O_4:Eu^{2+}$, Re^{3+} powders by various methods

Composition	Type of Combustion	Type of Fuel	Mixing	Combustion	Spectra		Ref.
					PL(nm)	PLE(nm)	
$SrAl_2O_4:Eu^{2+}$, Dy^{3+}, Tb^{3+}	Combustion	Urea	70°C – 4 h	400-900°C – 5 min	335	513	[1]
$Sr_{0.97}Al_2O_4$: $Eu_{0.01}$,$Dy_{0.02}$	Solution Combustion	Glycine		500°C – 3 min	242	513	[3]
$SrAl_2O_4:Eu^{2+}$, Dy^{3+},Gd^{3+}	Combustion	Urea	70°C – 4 h	600°C – 5 min	348	515	[4]
($Sr_{0.98}Eu_{0.02}$, $Dy_{0.04}$) Al_2O_4	Modified combustion	Urea		400-600°C – 5 min	337	529, 667	[5]
$SrAl_2O_4:Eu^{2+}$, Dy^{3+},0.10M Dy^{3+}& Eu^{3+}	Gel combustion synthesis	Urea + ammonium acetic	85°C	6000°C – 5 min	320	511	[6]
$Sr_{0.97-x}Al_2O_4$: $Eu^{2+}_{0.01}$, $Dy^{3+}_{0.02}$, Yb^{3+}_{x}	Solution Combustion	Urea	80°C – 2 h	600°C – 10 min	355	513	[7]
$Sr_{0.97}Al_2O_4$: $Eu_{0.01}$,$Dy_{0.02}$	Combustion	Urea	70°C – 4 h	540°C – 5 min	365	516	[8]

There are numerous publications discussing the combustion synthesis. The main goal of this research is to improve the properties of $SrAl_2O_4:Eu^{2+}$ by the combustion method with a lower combustion temperature in order to produce nanoparticle powder for different applications.

2. Experimental

2.1 Sample Preparation

$SrAl_2O_4:Eu^{2+}$ phosphor was prepared by combustion synthesis. The starting material included: aluminum nitrate ($Al(NO_3)_3.9H_2O$; Systerm, 98%), strontium nitrate ($Sr(NO_3)_2$; Aldrich, 99%), europium oxide (Eu_2O_3; Aldrich, 99.99%) and urea ($CO(NH_2)_2$; Systerm, 99%). Small amount of acid boric (H_3BO_3; Fisher, 100.04%) were used as flux and small amounts of urea were used as reducer and fuel. Figure 1 below shows the flow chart of $SrAl_2O_4:Eu^{2+}$ powders synthesis.

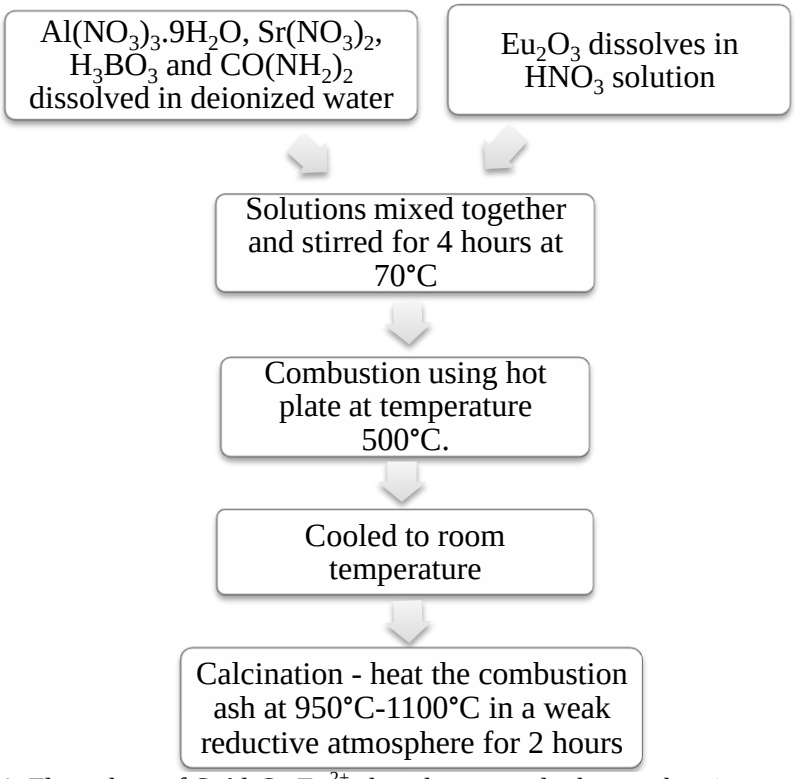

Fig.1. Flow chart of $SrAl_2O_4:Eu^{2+}$ phosphors powder by combustion synthesis.

There are four stages to describe the combustion synthesis.

Stage I: Composition of raw materials

The stoichiometric quantities of raw materials were calculated and weighed by using high precision mass balance. The composition of the acid boric was set as 0.08 mol %. Each raw material $Al(NO_3)_3.9H_2O$, $Sr(NO_3)_2$, H_3BO_3 and $CO(NH_2)_2$ was dissolved into 20 ml of deionized water to obtain a transparent solution. Wet mixing was used to obtain a homogeneous mixture. Deionized water is selected instead of distilled water due to the removal of the mineral ions, such as cations from sodium, calcium, iron, copper and anions from chloride and bromide, which will influence on the experiment result [11]. Eu_2O_3 was dissolved with a minimum amount of the HNO_3 solution to convert into $Eu(NO_3)_3$ according to the equation

$$Eu_2O_3 + 6HNO_3 \rightarrow 2\ Eu(NO_3)_3\ + 3H_2O \quad (1)$$

Stage II: Mixing

The two solutions were mixed together and stirred using a magnetic bar for several hours at 75°C to obtain a viscous gel solution. The mixing temperature was set in a range between 70°C to 80°C in this project due to several reasons. Firstly, according to the MSDS, aluminum nitrate has a fairly low melting point (73°C) but a high boiling point or decomposition temperature (135°C). The heating of aluminum nitrate above its melting point encourages the formation of a homogeneous solution. Furthermore, it can dissolve acid nitric which has a low boiling point (83°C).

Stage III: Combustion synthesis

The mixed viscous gel obtained continues for combustion reaction. In this project, combustion is done by using a hot plate instead of a furnace. White combustion ash was obtained in 3-5 min by combusting the precursor gel at a temperature of 500°C. Initially, the solution boiled and underwent dehydration followed by decomposition with emission of large amounts of gasses (oxides of carbon, nitrogen, and ammonia). Later, the viscous gels spontaneously start to burn and burn slowly without flame (smouldering combustion), thus producing white fine powder. The entire process takes less than 5 min. When heated at 500°C, the powder was held for a few minutes to ensure the combustion reaction was complete. The chemical equation of combustion is complicated and not yet verified; however, the brief equation can be shown as follows:

$$2Al(NO_3)_3.9H_2O + Sr(NO_3)_2 + CO(NH_2)_2 + Eu(NO_3)_3 + 1.5O_2 \rightarrow SrAl_2O_4 : Eu^{2+} + 20H_2O + 5N_2 + 14.5O_2 + CO_2 \quad (2)$$

Next, the combustion ash was cooled to room temperature.

Stage IV: Calcination step

The final pigment synthesis is done by heating the combustion ash at 950°C -1100°C in a weak reductive atmosphere for 2 h to obtain $SrAl_2O_4:Eu^{2+}$ phosphor. The weak reductive atmosphere was created by using a graphite crucible to inhibit further oxidation.

2.2 Characterization techniques

Phase identification was carried out using a Bruker, D8 Advance X-ray Diffraction (XRD) instrument with Cu-Kα radiation of a wavelength of 1.54 Å. Data were collected by step-scanning 2θ from 10° to 90° and 0.034 s counting time at each step at room temperature. The morphology and topography of the samples were observed by using a Zeiss Supra 35 VP scanning electron microscope (SEM). The samples were placed on the pin mount specimen holders with the help of a double-sided tape. The samples were coated with a few nanometer-thick gold palladium layer by using Sputter Coater Polaron SC 515 before SEM observation. Energy-dispersive X-ray spectroscopy (EDX) is known as a chemical microanalysis technique used with SEM. EDX was used to investigate the presence of elements of phosphors in a pre-captured SEM micrograph qualitatively and quantitatively.

The particle sizes of the samples were determined by a NANOPHOX (NX0064) Particle

Size Analyser. It used the photon cross-correlation spectroscopy (PCCS) technique for the simultaneous measurement of particle size and stability in a range of about 1 nm to 10 μm in opaque suspensions and emulsions. The key principle of PCCS is the 3D cross correlation technique based on dynamic light scattering. PCCS is using two separate beams with the same measuring volume for the illumination to create two separate speckle patterns. The time decay of the particles caused by Brownian motion is used to evaluate the size of nanoparticles and is shown in Fig. 2. The Brownian motion results from impacts of the thermal movement of the molecule in a suspending fluid.

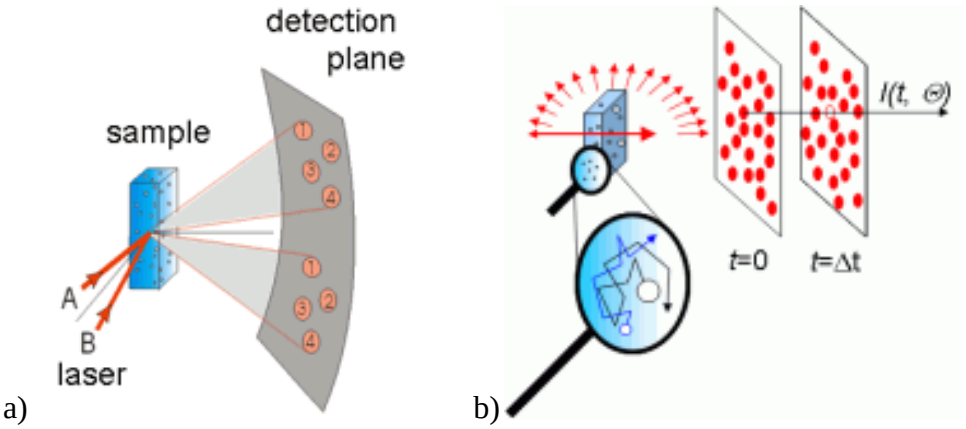

Fig. 2. (a) PCCS is using two separate beams with the same measuring volume to create two separate speckle patterns. (b) Brownian motion of the particles.

It is important to note that only singly scattered light is valid in evaluation of PCS theory. Any contribution of multiple scattered lights will affect the results and misinterpretations. Thus, PCS required highly diluted suspensions in order to avoid multiple scattering. Sensitivity will focus on the impurities in the liquid instead of the low concentration of particles. Very pure liquid and a clean room environment are required for the preparation and operation. For the sample preparation method, a small amount of the sample was dispersed in deionized water and stirred for 15 min using a magnetic bar. Then, it was vibrated for another 15 min by using an Ultrasonic bath.

3. Results and Discussion

3.1 X-ray Diffraction (XRD) analysis

XRD is a non-destructive analytical method used for identification and quantitative determination of the various crystalline forms (known as phase) present in samples. The phase identification is important because the phosphorescent powders properties are strongly dependent on the structure. Identification can be achieved by comparison of the XRD pattern – 'diffractogram' obtained from samples with an internationally recognized database. The diffractogram show the phases present (peak position), phase concentrations (peak heights), amorphous content (background bump), and crystalline size/strain (peak width).

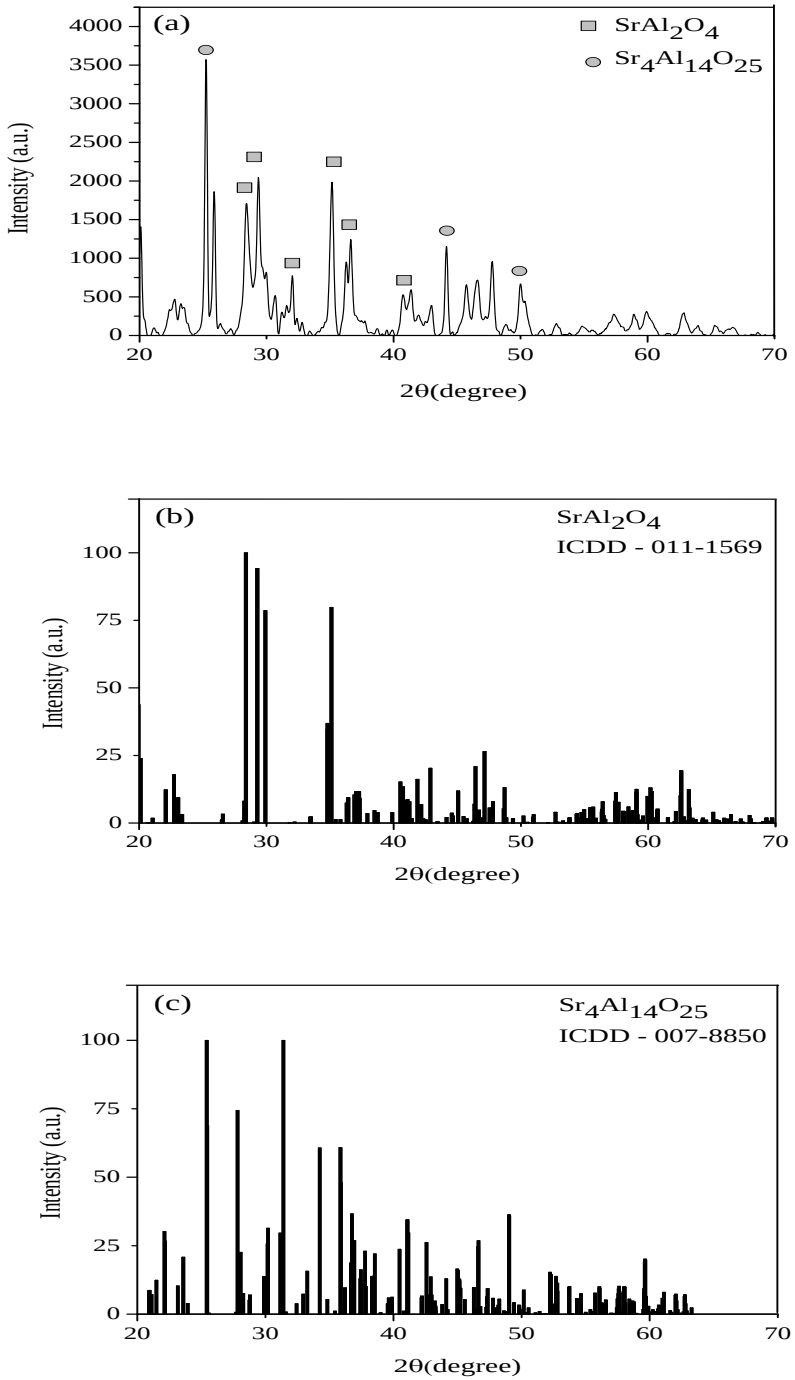

Fig. 3. (a) XRD for $SrAl_2O_4$:Eu^{2+}, (b) theoretical XRD for monoclinic $SrAl_2O_4$ taken from ICDD file no. 011-1569 and (c) orthorhombic $Sr_4Al_{14}O_{25}$ taken from ICDD file no. 007-8850.

A typical X-ray diffraction pattern of the stoichiometric $SrAl_2O_4$: Eu^{2+} powder prepared at 1000°C in a graphite crucible is shown in Fig. 3. We can observe that the product of combustion is multiphase and contains characteristic peaks of monoclinic $SrAl_2O_4$ phase as a major phase and

orthorhombic $Sr_4Al_{14}O_{25}$ as a secondary phase. The different peaks can be indexed to the $SrAl_2O_4$ (ICSD - 011-1569) and $Sr_4Al_{14}O_{25}$ (ICSD - 007-8850) (ICSD: inorganic crystallographic structure database). No other products or starting materials are observed, which shows that a small amount of doped rare earth ions does not influence the $SrAl_2O_4$ phase composition.

3.2 SEM analysis

Microscopy and topography analysis on phosphorescent powders was done through scanning electron microscopy (SEM). The main idea is to observe any crystallize phases present in the samples.

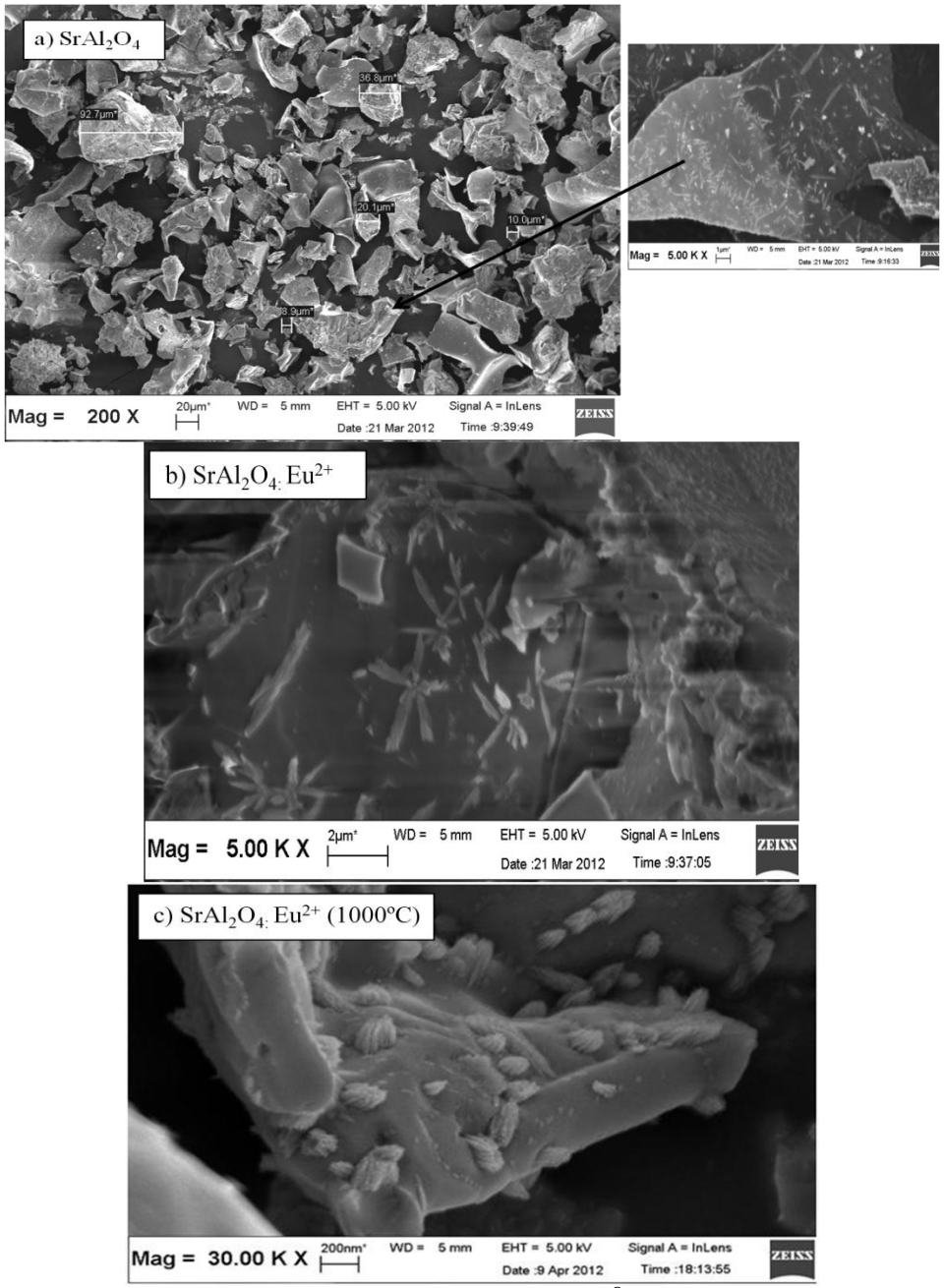

Fig.4. a) Sample $SrAl_2O_4$ before calcinations, b) Sample $SrAl_2O_4$: Eu^{2+} before and c) after calcinations at temperature 1000°C.

Figure 4a depicts the morphology of the host material $SrAl_2O_4$ without adding any activator and co-activator, while Figs. 4b and 4c show the $SrAl_2O_4$:Eu^{2+} samples with an addition of europium activator. Figure 4a represents the particle size distribution obtained from SEM for sample $SrAl_2O_4$ before calcinations. It is evident from the figure that an irregular structure at various sizes and lengths was obtained. All the samples show the formation of crystal structures of phosphor. The homogenous distribution and size of a star-like structure on the matrix surface shows the activator ions were homogenously dispersed throughout the phosphor matrix. In the case with an additional amount of Eu, sample $SrAl_2O_4$: Eu^{2+} (Fig. 4 (b)) has higher crystallite or star-like particles compared to sample $SrAl_2O_4$. The particles connected together form a larger network of star-like structure. The crystal structure has a clear, longer, and equal size in each leg of the star-like particles. After calcinations at 1000°C with 2-h soaking, the structure of the star-like particles of sample $SrAl_2O_4$: Eu^{2+} are closed and stacked together to form a flower-like structure with a better crystal (Fig. 4(c)).

The possible mechanism of the flower-like structure can be described as shown in Fig. 5. Generally, the crystal growth process involves two parts: nucleation and growth. The particles undergo nucleation at the initial state. With an increase in temperature, the grains become compressed and finer. The needle shape and star-like structure appear after 500°C. This structure is unstable and agglomerates during calcinations at 1000°C to form a stable specific flower-like structure [12, 13].

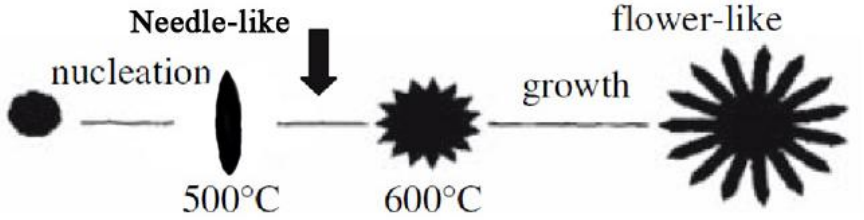

Fig. 5. Scheme to illustrate the possible mechanism of the flower-like structure of $SrAl_2O_4$: Eu^{2+} [12].

3.3 Energy-dispersive X-ray Spectroscopy (EDX) Analysis

EDX is used to characterize the elemental composition of the phosphor powder. The EDX results in Table 2 indicate the presence of a small amount of europium for sample $SrAl_2O_4$: Eu^{2+}.

Table 2. Overall EDX results of sample $SrAl_2O_4$, $SrAl_2O_4$: Eu^{2+} (before calcinations) and $SrAl_2O_4$: Eu^{2+}, annealed at 1000°C

Samples / Element	**Al**		**Sr**		**Eu**		**O**	
	Wt%	**At%**	**Wt%**	**At%**	**Wt%**	**At%**	**Wt%**	**At%**
$SrAl_2O_4$	26.22	23.35	32.19	08.83	-	-	10.78	21.57
a) $SrAl_2O_4$: Eu^{2+}	27.92	24.94	30.00	08.25			35.29	53.17
b) $SrAl_2O_4$: Eu^{2+} (after)	19.92	24.96	49.18	18.98	04.88	01.09	26.02	54.98

Table 2 shows that the content of aluminum is stable throughout the combustion and calcinations processes. The content of the europium element is examined after calcination and indicates that the content of europium distributed to the grain boundary phase and grain surface diffuse into the host lattice by rapid grain boundary diffusion [14]. The oxygen content increases upon the addition of europium in the sample and is very high, which can be due to the large amount of oxygen supplied during combustion and calcinations processes. No carbon and

nitrogen are present in the EDX analysis, which indicates that the combustion synthesis is complete.

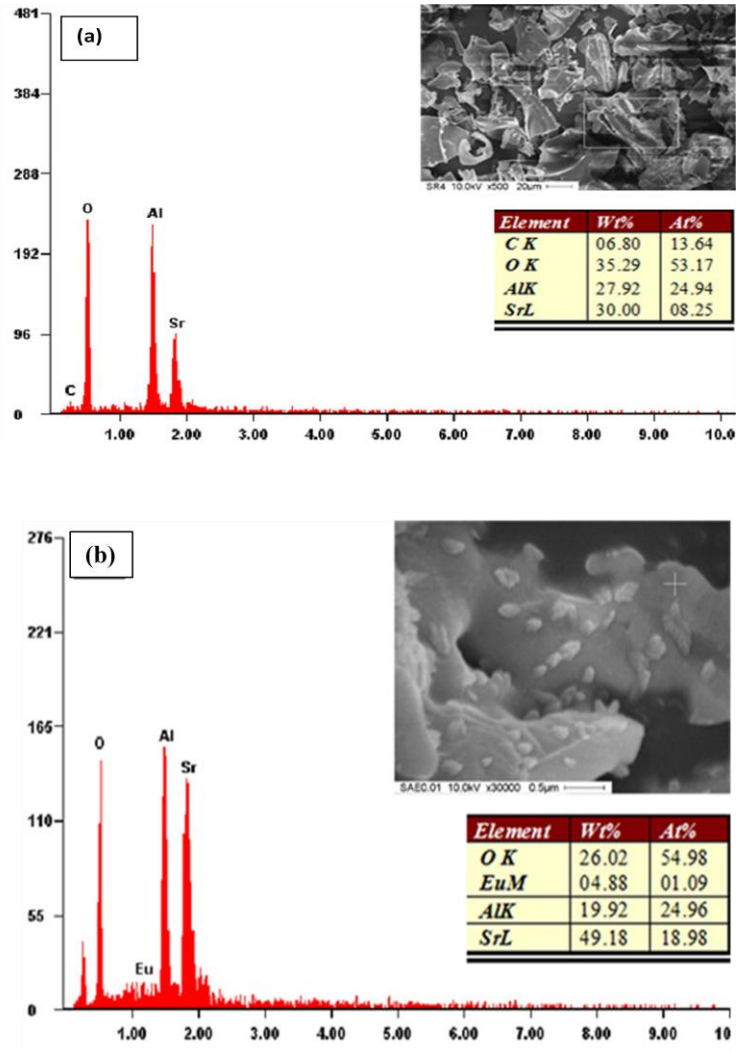

Fig. 5. EDX results of sample $SrAl_2O_4$: Eu^{2+} before (a) and after calcination (b).

3.4 Particle size analysis

The particle size of the samples was measured to justify the presence of a nanosize powder in this project. Table 3 below shows the particle analysis for samples $SrAl_2O_4$ (after calcinations) and $SrAl_2O_4$: Eu^{2+} before and after calcinations. The average size, x_{50} will be used as a reference.

Table 3. Particle size analysis data for samples $SrAl_2O_4$ and $SrAl_2O_4$: Eu^{2+} before and after calcinations

Samples	**x_{10} (nm)**	**x_{50} (nm)**	**x_{90} (nm)**	**SMD (nm)**	**VMD (nm)**
$SrAl_2O_4$	81.19	84.14	89.39	84.54	84.61
$SrAl_2O_4$: Eu^{2+}	44.15	51.62	60.02	51.27	51.98
$SrAl_2O_4$: Eu^{2+} (after)	112.65	132.21	154.26	131.29	133.20

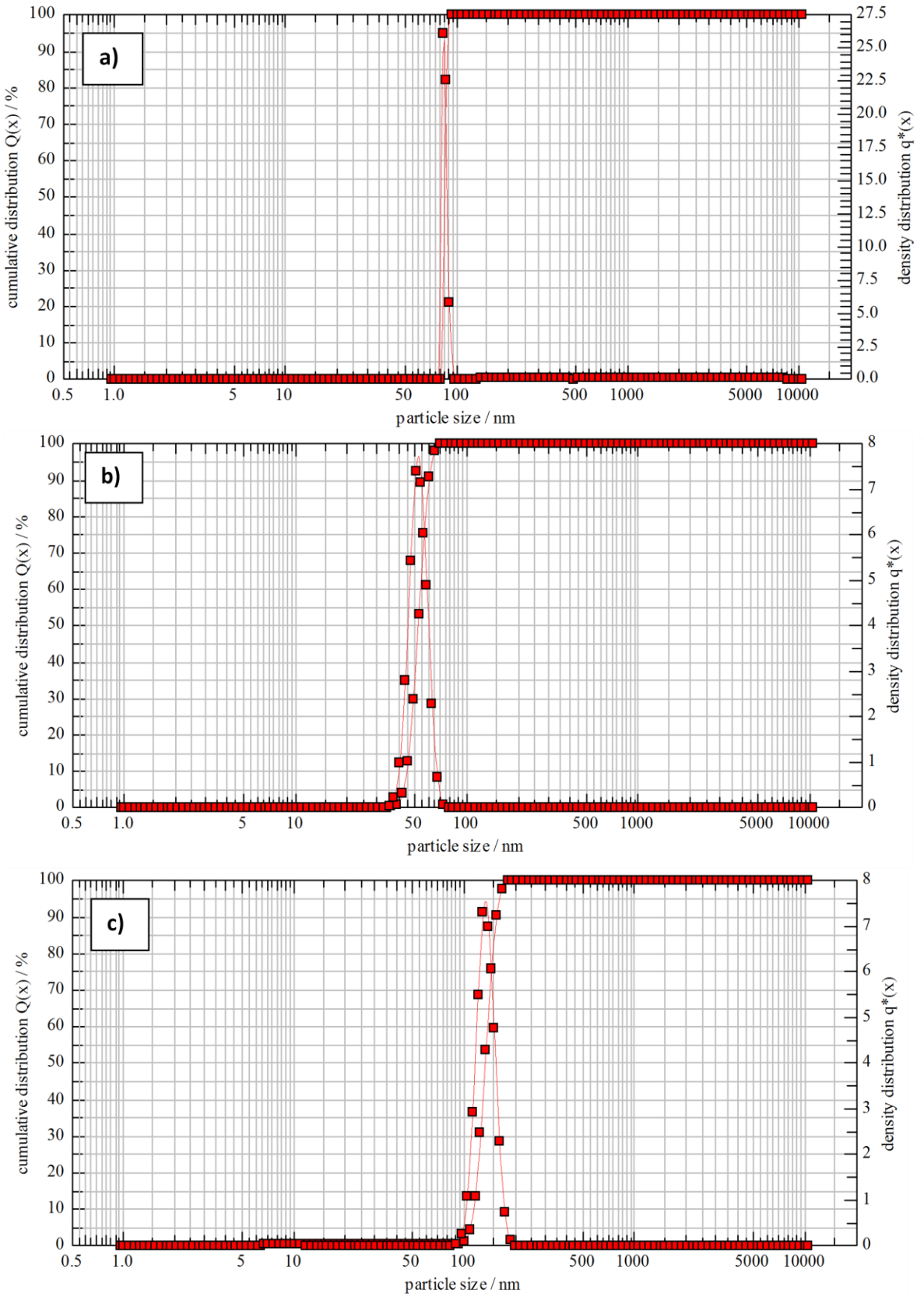

Fig. 6. Graph of particle size analysis for sample a) $SrAl_2O_4$, b) $SrAl_2O_4$: Eu^{2+} before and c) $SrAl_2O_4$: Eu^{2+} after calcinations.

The results show that all the samples achieve nanoparticle size except for sample $SrAl_2O_4$: Eu^{2+} after calcination. The particle size ranges from 81 to 89 nm for $SrAl_2O_4$, while for $SrAl_2O_4$:Eu^{2+}, it is 44 to 60 nm before the calcination processes take place. This can be explained from SEM analysis where europium was homogeneously dispersed throughout the phosphor matrix to produce a crystalline phase. The crystalline formation helps to produce a powder with a finer particle size. Furthermore, we should emphasize that the particle size distribution for $SrAl_2O_4$ has a narrow range which does not exceed 10 nm compared to $SrAl_2O_4$: Eu^{2+}. However, for sample $SrAl_2O_4$: Eu^{2+} after calcination, we observed an increase in the particle size after heating at a higher temperature due to grain grow. Excessive sintering and aggregation of particles occurs, and thus the particle size increases.

There is another method which can be used to determine the particle size. XRD pattern parameters were used to determine the average particle size by using Scherrer equation: $D_{hkl}=k\lambda / (\beta\cos\theta)$, where D_{hkl} is the size of the crystal particles, k is equal to 0.89, β is the full-width at half maximum (FWHM), and θ is the Bragg angle that corresponds to the peak analyzed. The XRD results were used to compare with the particle size PCCS analysis. Figure 7 shows one of the parts taken from the XRD data from 28 to 36 degree. The particle size of each peak was calculated as shown in the equation below, and it indicates an average grain diameter of the particles.

$$D_1 = \frac{k\lambda}{(\beta_1 \cdot \cos\theta_1)} = \frac{0.89 \times 0.15405\text{nm}}{\left(\frac{0.2534 \cdot \pi}{180}\right) \cdot \cos(14.209)} = 31.79\ \text{nm}$$

$$D_2 = \frac{k\lambda}{(\beta_2 \cdot \cos\theta_2)} = \frac{0.89 \times 0.15405\text{nm}}{\left(\frac{0.1807 \cdot \pi}{180}\right) \cdot \cos(14.677)} = 44.64\ \text{nm}$$

$$D_3 = \frac{k\lambda}{(\beta_3 \cdot \cos\theta_3)} = \frac{0.89 \times 0.15405\text{nm}}{\left(\frac{0.3374 \cdot \pi}{180}\right) \cdot \cos(17.575)} = 48.40\ \text{nm}$$

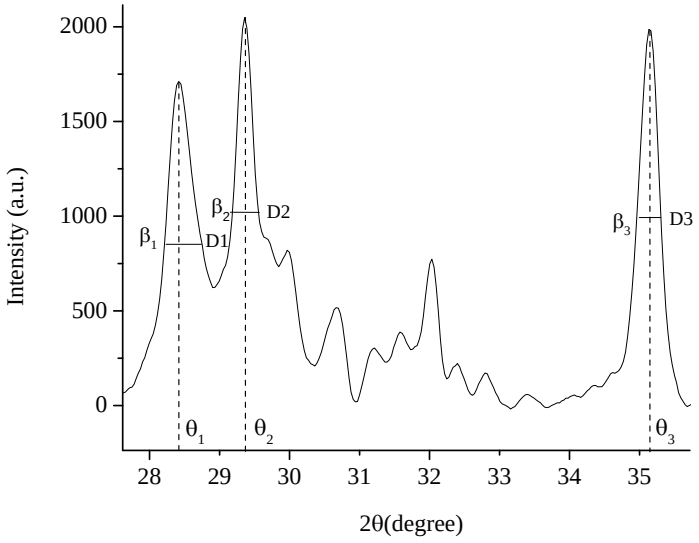

Fig. 7. Particle size of sample $SrAl_2O_4$: Eu^{2+} (1000°C) estimated from XRD measurement.

The particle sizes calculated from the Scherrer equation are in the range of 31 to 48 nm. It

has lower values compared to the results obtained using a Nanophox particle size analyzer. By comparing both methods, particle size calculated is approximate with the result obtained from Nanophox, which is more accurate referring to the grain growth when temperature is increased.

4. Conclusions

$SrAl_2O_4:Eu^{2+}$ phosphor was successfully synthesized by combustion at 500°C with calcinations at 1000°C under a reductive atmosphere. The characteristic peaks of monoclinic $SrAl_2O_4$ (ICDD - 011-1569) phase as a major phase and orthorhombic $Sr_4Al_{14}O_{25}$ (ICDD - 007-8850) as a secondary phase were obtained from X-ray diffraction analysis. No other products or starting materials are observed, which shows that a small amount of doped rare earth ions does not influence the $SrAl_2O_4$ phase composition. For scanning electron microscopic analysis, homogenous distribution and size of the flower-like structure on the matrix surface was observed; this shows that the activator ions were homogenously dispersed throughout the phosphor matrix leading to the higher excitation and emission. The particle-size analysis results implied that the phosphor powder has an average size of 50 nm before and 132 nm after calcinations. The applied combustion synthesis and calcination at low temperatures in comparison with traditional methods give promising results, and nanosized phosphors with improved properties can find a large application.

Acknowledgements

Financial support is acknowledged from Final Year Project, University Sains Malaysia, and Post Graduate Grant Research under grant no. 1001/PBAHAN/8044033.

References

[1] H. Song, and D. Chen, J. Lumin., 22 (6), 554, (2007).
[2] E. Shafia, M. Bodaghi, and M. Tahriri, Curr. Appl Phys., 10 (2), 596 (2010).
[3] T. Peng, H. Yang, et al., Mater. Lett., 58 (3), 352 (2004).
[4] H. Song, D. Chen, et al., Displays, 29 (1), 41 (2008).
[5] H. Chander, D. Haranath, et al., J. Cryst. Growth, 271 (1), 307 (2004).
[6] R. Zhang, G. Han, et al., Mater. Chem. Phys., 113 (1), 255 (2009).
[7] R. Chen, Y. Wang, et al., J. Lumin., 128 (7), 1180 (2008).
[8] S. Nguyen Manh, V. Le Thi Thao, et al., J. Phys. Conf. Ser., 187 (1), 012017 (2009).
[9] K.C. Patil, S.T. Aruna, and T. Mimani, Curr. Opin. Solid State Mater. Sci., 6 (6), 507 (2002).
[10] X. Yu, C. Zhou, et al., Mater. Lett., 58 (6), 1087 (2004)
[11] J.J. Moore and H.J. Feng, Prog. Mater Sci., 39 (4). 243 (1995).
[12] H. Ji, G. Xie, et al., J. Sol-Gel Sci. Technol., 44 (2), 133 (2007).
[13] P. Zhang, M. Xu, et al., J. Sol-Gel Sci. Technol., 43 (1), 59 (2007).
[14] Y.Liu, and C.-N. Xu, J. Phys. Chem. B, 107 (17), 3991 (2003).